

Proceedings of the International Conference "Condensed Matter Physics", Jaszowiec 2000

PHOTOEMISSION ELECTRONIC STATES OF THALLIUM- AND BISMUTH-BASED SUPERCONDUCTORS

R. ZALECKI^a, A. KOŁODZIEJCZYK^a, J.W. KÖNIG^b AND G. GRITZNER^b

^aUniversity of Mining and Metallurgy, Faculty of Physics and Nuclear Technique
Al. A. Mickiewicza 30, 30-059 Cracow, Poland

^bJohannes Kepler Universität, Institut für Chemische Technologie Anorganischer Stoffe
4040 Linz, Austria

X-ray photoemission spectra the core-levels as well as the X-ray photoemission spectra and ultraviolet photoemission spectra from the valence bands of the $(\text{Tl}_{0.6}\text{Pb}_{0.5})(\text{Sr}_{0.9}\text{Ba}_{0.1})\text{Ca}_2\text{Cu}_3\text{O}_y$ and $(\text{Bi}_{1.75}\text{Pb}_{0.35})\text{Sr}_{1.9}\text{Ca}_{2.05}\text{Cu}_{3.05}\text{O}_y$ superconductors were measured and analyzed. Special attention was paid to the valence band X-ray photoemission spectra and ultraviolet photoemission spectra, the Cu $2p$ core-level X-ray photoemission spectra and the Cu $L_{2,3}-M_{4,5}M_{4,5}$ and O $K-L_{2,3}L_{2,3}$ Auger spectra. Both Cu $2p_{3/2}$ and Cu $2p_{1/2}$ core-level lines consisted of two spin-orbit split main lines accompanied with the two satellite lines. The charge transfer energy Δ from the oxygen ligand to the copper $3d^9$ states and the hopping integral t were estimated from the energy separation between the main line and the satellite line taking advantage of the local cluster model calculations and their extension to high-temperature superconductors. The Coulomb correlation on-site energy U_{dd} of two electrons in the same copper orbital and U_{pp} of two electrons in the oxygen orbital as well as the correlation energy U_{cd} of the $2p$ core hole - $3d$ electron interaction have been estimated from the Auger electron spectra and the valence band spectra. They are: $U_{dd} = 6.0 \pm 0.5$ eV, of $U_{pp} \cong 10 \pm 1$ eV and of $U_{cd} \cong 8.0 \pm 0.5$ eV nearly the same for both the Tl- and Bi-compounds. We conclude that these compounds are the charge transfer strongly-correlated metals.

PACS numbers: 74.72.-h, 79.60.-i

1. Introduction

The presence of electron correlations in high-temperature superconductors (HTS) is the one among others most important effect in these materials. Physical properties like magnetism in strongly correlated systems, heavy fermion behavior, giant magnetoresistance, etc. are governed by strong electron-electron interactions. The one - electron Bloch-like theory is insufficient to describe their physical

properties. Solids are many-electron systems and the electrons interact with each other via the Coulomb and exchange interaction. To understand the nature of HTS it is important to have knowledge of their correlated electronic states. Photoelectron spectroscopy (PES) is one of the most important tool to probe these electronic states. The basic problem with the interpretation of the d -electron photoemission in HTS stems from the fact of large correlation effect among $3d$ electrons and the hybridization of the metal d -electrons with the ligand p -electrons.

The theory of the electronic structure in the transition metal (TM) compounds was developed in [1–5]. The basic electronic features of TM compounds were described by the so-called Zaanen, Sawatzky and Allen phase diagram [2] U_{dd}/t versus Δ/t . U_{dd} is the d – d on-site electron (hole) Coulomb correlation energy (Hubbard energy), Δ is the charge transfer energy for the excitation of an electron from a ligand ion onto the d -hole state of metal ion, t is the hybridization term between p and d states (effective hybridization term T_{eff}), sometime called the transfer integral, associated with the p – d Coulomb correlation energy U_{cd} between $2p$ core hole and $3d$ holes. This theory included the correlation and hybridization effects.

One would normally expect the U_{dd} to increase and the bare charge-transfer Δ to decrease for the TM compounds with higher atomic numbers. As estimated from calculations [6] and electron-spectroscopy studies [7] the one-site Coulomb correlation energy is known to be large for the late TM and their compounds.

The dominating ground states in the investigated samples are one-hole states and the two-hole states are the minority. In the photoemission the local cluster model calculations were thoroughly used [8–13]. The model assumes in copper oxides the existence of separated $(\text{CuO}_6)^{10-}$ cluster and it describes the copper $3d$ electrons hybridized to the oxygen $2p$ states. The ground states are assumed as a linear combination of the d^9 and $d^{10}L^{-1}$ configurations. The final states in the copper $2p$ photoemission are the linear combination of $2p^53d^9$ and $2p^53d^{10}L^{-1}$ configurations. From this approach one can elaborate the photoemission spectra and estimate the U_{cd} , Δ , and t values. Especially, the satellite to main peak energy distance ΔE_{M-S} in the Cu $2p$ core-level X-ray photoemission spectra (XPS) was expressed in [8–10, 14] as a function of the U_{cd} , Δ , and t .

Also the structure of the Cu $L_{2,3}$ – $M_{4,5}M_{4,5}$ Auger line for copper compounds may be analyzed according to the model presented in [8]. In the present paper the quantitative estimates of the U_{dd} as well as the U_{pp} , which is the on-site Coulomb correlation energy of two electrons (holes) in the oxygen orbital, were made from the relevant Auger lines and the “copper” and “oxygen” parts of the valence band.

For the high-temperature superconductors a lot of photoemission and Auger electron spectroscopic studies have been reported up to now [15–27]. Among them the most important resonant photoemission valence band spectra and the angle resolved photoemission in the binding energy region close to the Fermi surface have been carried out [14, 17–25].

It is already well-established that the high-temperature superconductivity appears due to doping by holes like in $\text{YBa}_2\text{Cu}_3\text{O}_{7-\delta}$ or by electrons like in $\text{Nd}_{2-x}\text{Ce}_x\text{CuO}_{4-y}$. In the former system the charge neutrality requires the con-

version of Cu^{2+} to Cu^{3+} or the converting O^{-2} ($2p^6$) to O^{-1} ($2p^5$). It means an appearance of holes L^{-1} in the oxygen $2p$ band (L^{-1} indicates an oxygen ligand hole state) yielding the formally trivalent copper Cu^{3+} instead of the real Cu^{3+} ($3d^8$) states. It was proved that the superconductivity is determined by the formally trivalent copper Cu^{3+} with the $3d^9L^{-1}$ electronic states, usually called formally trivalent copper because the extra electron missing with respect to divalent copper Cu^{2+} is taken from the oxygen $2p$ reservoir rather than from the Cu $3d$ reservoir [15-27].

The valence band (VB) states are a mixture of ligand (L) p -states and metal d -states and thus can be written as d^9L states. This valence band leads to two final states after photoemission, namely d^8L and d^9L^{-1} . The first state corresponds to the creation of a d^8L state (e.g. $\text{Cu}^{3+} 3d^82p^6$) out of d^9L state (e.g. $\text{Cu}^{2+} 3d^92p^6$ in CuO) which requires a correlation energy U_{dd} . The second final state d^9L^{-1} ($3d^92p^5$) is produced by a p -ligand to d -metal charge transfer out of the photoionized state d^8L due to hybridization. It needs a charge transfer energy Δ . Thus two types of electronic excitations are possible in VB of transition metal oxides. The first excitation of d -electron from TM ion and its transfer to another distant transition metal ion which are governed by the energy U_{dd} . The second excitation is the transfer of a ligand electron onto a transition metal ion described by the energy Δ . The relative magnitude of these two energies U_{dd}/Δ defines whether a compound is a *Mott insulator* (MI) ($U_{dd} < \Delta$) (or more generally, a *Mott compound*) or a *charge-transfer compound* (CTC) ($U_{dd} > \Delta$).

In the present paper the XPS and ultraviolet photoemission spectra (UPS) of the $(\text{Tl}_{0.6}\text{Pb}_{0.5})(\text{Sr}_{0.9}\text{Ba}_{0.1})_2\text{Ca}_2\text{Cu}_3\text{O}_y$ and $(\text{Bi}_{1.75}\text{Pb}_{0.35})\text{Sr}_{1.9}\text{Ca}_{2.05}\text{Cu}_{3.05}\text{O}_y$ superconductors were measured and analyzed. Special attention was paid to the valence band XPS/UPS, the Cu $2p$ core-level XPS and the Cu $L_{2,3}$ - $M_{4,5}$ and O K - $L_{2,3}$ Auger spectra to estimate the all energies and parameters characterizing the electron correlation effects in a consistent way for the first time.

2. Experimental

Polycrystalline pellets of the $(\text{Tl}_{0.6}\text{Pb}_{0.5})(\text{Sr}_{0.9}\text{Ba}_{0.1})_2\text{Ca}_2\text{Cu}_3\text{O}_y$ and $(\text{Bi}_{1.75}\text{Pb}_{0.35})\text{Sr}_{1.9}\text{Ca}_{2.05}\text{Cu}_{3.05}\text{O}_y$ superconductors were prepared by solid-state reaction with the superconducting transition temperature T_{c0} of 118 K and 103 K, respectively, by a procedure described elsewhere [28-30].

We employed a system XPS/UPS (ultraviolet) Leybold LHS10 equipped with the dual Al- and Mg- K_α X-ray sources with a typical resolution of 0.85 eV and with the high intensity UV source with the energy resolution of about 50 meV. As a test of contamination - free surface the intensity of carbon C $1s$ typical peak at about 298 eV was used prior to experiment under the vacuum better than 10^{-9} Torr. The C $1s$ signal due to carbonate impurities was negligible for all samples. The spectrometer was calibrated using the Ag Fermi edge, the Ag $3d_{5/2}$ line and the Cu $2p_{3/2}$ white line to which the binding energies 0 eV, 368.3 eV, and 932.7 eV were assigned, respectively. The experiments were performed also at the LN₂ temperature for comparison and to avoid surface degradation. The cleanliness of sample surface was ensured by *in situ* scraping with a diamond file.

3. Results and their analysis

The full energy range spectra in room temperature are shown in Fig. 1 with the indicated important photoemission lines.

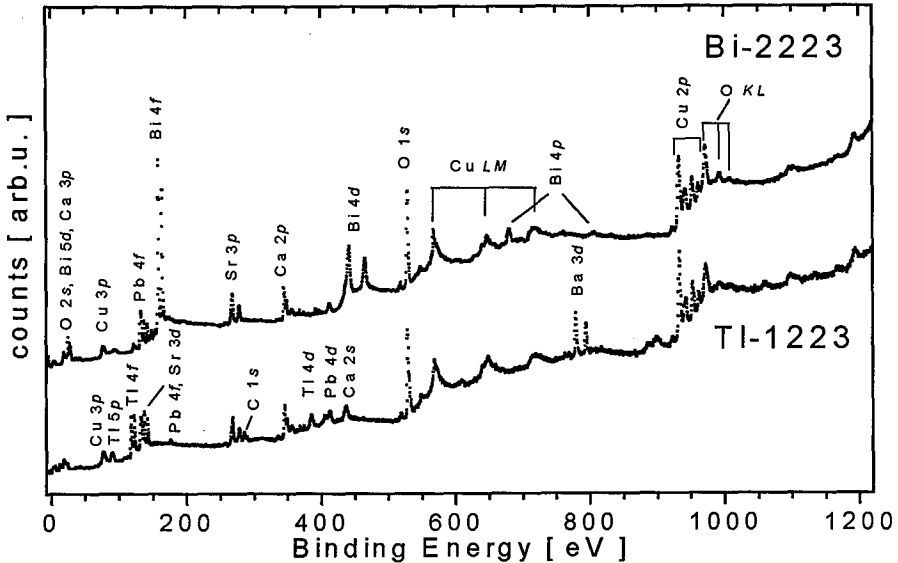


Fig. 1. The full scan XPS ($Al-K\alpha$) of the $(Bi_{1.75}Pb_{0.35})Sr_{1.9}Ca_{2.05}Cu_{3.05}O_y$ (Bi-2223) and $(Tl_{0.6}Pb_{0.5})(Sr_{1.9}Ba_{0.1})_2Ca_2Cu_3O_y$ (Tl-1223) superconductors with the important lines indicated.

Figure 2 shows the $Cu\ 2p_{3/2}$ and $2p_{1/2}$ XPS ($Al-K\alpha$, 1486.6 eV) core-level spectra in room temperature. They exhibit the main lines M at 932.5 eV ($J = 3/2$) and at 952.5 eV ($J = 1/2$), respectively.

In the $Cu\ 2p$ core-level spectra the broad satellites S_1 and S_2 appear at the 941.9 eV and at 961.6 eV binding energy, respectively, in addition to the spin-orbit split main lines M_1 and M_2 sometime with the additional structure. The satellites are characteristic of other insulating cuprates [14, 32] with Cu^{2+} ions with $S = 1/2$ spins. The satellite results from the multiplet splitting effects due to the interaction between the $2p$ core hole and the $3d^9$ electronic configuration in the final state of the photoemission process [31, 32]. In the core $Cu\ 2p$ spectrum the energy difference between the main M_1 and satellite S_1 peak is about 1 eV larger than in other insulating cuprates [14, 32] which means a larger charge transfer energy t between $2p$ and $3d$ holes. It was established that the M line occurs for significant different energy for different compounds while the satellite has roughly the same binding energy in all compounds [14]. The final state configurations of the main and satellite lines are labelled in Fig. 2.

Generally speaking, in the ground state the copper oxides with the Cu^{2+} ions have one hole in the d -shell ($3d^9$ configuration) and a filled ligand shell L .

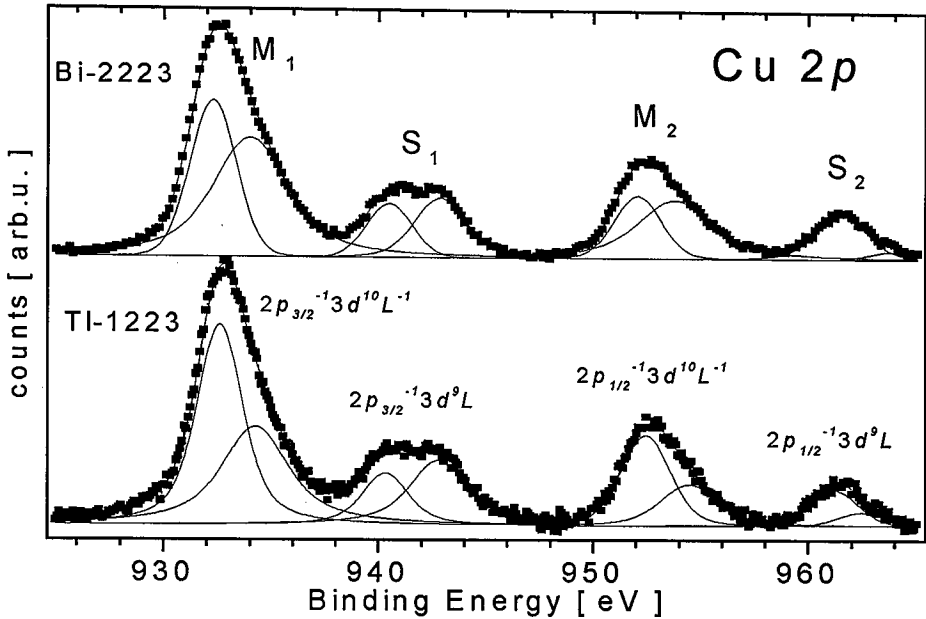


Fig. 2. The Cu 2*p* core-level spectra of the $(\text{Bi}_{1.75}\text{Pb}_{0.35})\text{Sr}_{1.9}\text{Ca}_{2.05}\text{Cu}_{3.05}\text{O}_y$ (Bi-2223) and $(\text{Tl}_{0.6}\text{Pb}_{0.5})(\text{Sr}_{0.9}\text{Ba}_{0.1})_2\text{Ca}_2\text{Cu}_3\text{O}_y$ (Tl-1223) superconductors after subtraction of the background, with the best fitted lines (solid lines) and with the final state configurations as indicated.

The notation is $3d^9L$ and refers to the Cu^{2+} ion and L represents the fully occupied oxygen $2p$ shell ($2p^6$ configuration). The photoexcitation in the Cu $2p$ shell leads to two final states: one, where after creation of the $2p$ core hole the ground state configuration $3d^9L$ is left roughly intact; another one, where one electron is transferred from the ligand shell L into the d -shell due to relaxation process, leading to a $3d^{10}L^{-1}$ configuration. The latter configuration applies to the M line and hence the binding energy is: $E_M = E(c^{-1}d^{10}L^{-1}) \cong E(c^{-1}d^{10}) + E(L^{-1})$ where c^{-1} indicates core hole in Cu $2p$ shell. By the same reasoning the S line is described by energy $E_S = E(c^{-1}d^9L)$. Thus, the main line energy is different because is influenced by a strong correlation with the ligand in the sense that the production of a hole in the ligand valence band orbital depends on the ligand ion. This is not the case for S line. In the ground state of TM compounds the $3d$ valence shell is usually in energy above the ligand valence orbitals. However, the additional Coulomb interaction U_{cd} may pull it below the top of the ligand valence band. This is the case in HTS. This is an unstable situation which does not correspond to the ground state but to the satellite. It is then energetically possible to transfer an electron from the ligand band into the empty $3d$ orbital and the ion attains its ground state. In such a case the initial state configurations for Cu are $3d^9L$ and $3d^{10}L^{-1}$ with some mixing. These configurations correspond to two states of which one is filled (mostly $3d^9L$) and the other is empty (mostly $3d^{10}L^{-1}$) in the initial state. These two states can be populated in the final state creating a

main M line (mostly $3d^{10}L^{-1}$) and a satellite S line (mostly $3d^9L$). That is why the fits were made with two lines as shown in Fig. 2 subtracting the background according to the Tougaard procedure [33]. The combination of the Lorentzian and Gauss line was fitted to the experimental data of the Cu $2p$ core level spectra.

Figure 3 shows the room and liquid nitrogen temperature XP and UP spectra of the valence bands of both superconductors. The spectra are very similar for both superconductors with exception that the Fermi edge E_F for polycrystalline material is only observed for Bi-2223 specimen. The edge is a very good zero reference point for calibration of energy scale in further analysis of the photoemission spectra. It was already established that the O $2p$ states participate in VB mostly close to the Fermi level whereas the Cu $3d$ states are contributing to the bottom of VB [14–19]. Therefore, the position of the leading $2p$ emission is at -2.7 eV below E_F and of the $3d$ emission is at -5.1 eV below E_F as roughly estimated with two lines fitting shown in Fig. 3. These energy values will be used to analyze the relevant Auger lines together with the VB spectrum of Bi-2223 in the next paragraph.

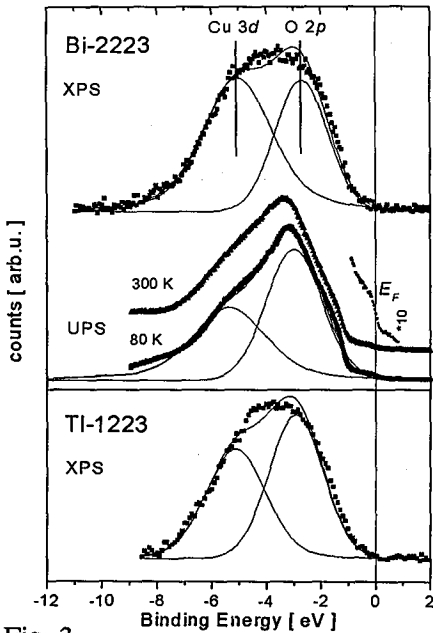


Fig. 3

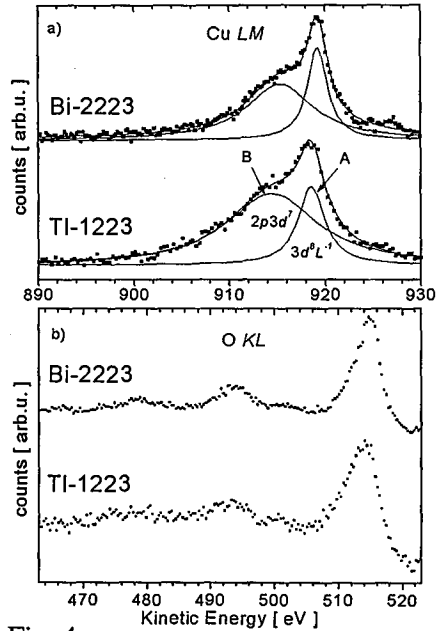


Fig. 4

Fig. 3. The X-ray photoemission ($Mg-K_{\alpha}$) and ultraviolet photoemission (He-I) spectra. The Cu $3d$ and O $2p$ emissions together with the Fermi edge in Bi-2223 UPS spectra are shown.

Fig. 4. Auger electron lines (a) of Cu: $L_{3-M_{4,5}}M_{4,5}$ and (b) of O: $K-L_{2,3}L_{2,3}$ with the final state configurations for copper as indicated.

The Cu $L_{2,3-M_{4,5}}M_{4,5}$ Auger lines of $M_{4,5}M_{4,5}$ and of O $K-L_{2,3}L_{2,3}$ in room temperature are shown in Fig. 4. The Cu $L_{2,3-M_{4,5}}M_{4,5}$ Auger line for both superconductors consists of the main high-kinetic energy component (A) at

$E_A = 919.2$ eV and the second lower-kinetic energy component (B) at $E_B = 915.3$ eV as estimated after fitting two lines to the measured spectrum and after subtraction of the background according to the Tougaard procedure [33]. The line A was attributed to the $3d^8L^{-1}$ final state configuration after the Auger process starting from a $2p_{3/2}3d^{10}L^{-1}$ intermediate state. The line B was assigned to the $3d^7$ final configuration from a $2p_{3/2}3d^9$ intermediate state [8].

The energy positions of the XPS Cu $2p$ lines, of the Auger lines and of the Cu $3d$ and O $2p$ emission from XPS valence bands as taken from the experimental spectra and from the fitting procedures are collected in the Table.

TABLE

The experimental and fitted energy positions [eV] of the Cu $2p$ and Auger lines together with the valence band energy positions of the Cu $3d$ and O $2p$ emissions. (The estimated maximal error of the values given in the Table is about 0.2 eV.)

		XPS		XPS		Auger lines*			Valence band	
		Cu $2p_{3/2}$		Cu $2p_{1/2}$		(I)		(II)	Cu $3d$	O $2p$
		E_{M1}	E_{S1}	E_{M2}	E_{S2}	E_A	E_B	E_A		
Bi- 2223	Exp.	932.5	941.1	952.5	961.6	919.1	914.5	514.8	-3.5	-3.5
	Fit	932.3	940.5	952.1	961.6	919.2	915.3	—	-5.1	-2.7
Tl- 1223	Exp.	932.7	940.9	952.6	961.5	918.2	913.7	514.2	-3.8	-3.8
	Fit	932.6	940.3	952.4	961.2	918.5	914.4	—	-5.1	-2.9

* (I) — Cu $L_{2,3}-M_{4,5}M_{4,5}$, (II) — O $K-L_{2,3}L_{2,3}$

3.1. Analysis of Auger lines together with the valence band

In order to estimate the Coulomb correlation strength U_{dd} and U_{pp} one can use Auger electron lines of Cu $L_{3-}M_{4,5}M_{4,5}$ at about 919 eV and of O $K-L_{2,3}L_{2,3}$ at about 515 eV shown in Fig. 4. The spectral features do not significantly change for both superconductors indicating very similar Coulomb correlation energies, U_{dd} as well as U_{pp} , in these compounds. In order to extract a quantitative estimate of U_{dd} , we have compared the Cu $L_{2,3-}M_{4,5}M_{4,5}$ Auger spectrum with the self-convoluted density of states (DOS) after aligning them to the respective Fermi energies $E_F = 0$. To do this we have followed the procedure presented in [34]. The position of relevant Auger line was compared with the self-convoluted DOS of the XP spectra of the valence band taking into account that the O $2p$ states participate in VB mostly close to the Fermi level E_F whereas the Cu $3d$ states are contributing to the bottom of VB (see Fig. 3). The peak at -2.7 eV below E_F is primarily due

to the oxygen 2*p* emission and the peak at -5.1 eV below E_F comes mainly from the copper 3*d* emission [14–29]. The procedure is shown in Fig. 5.

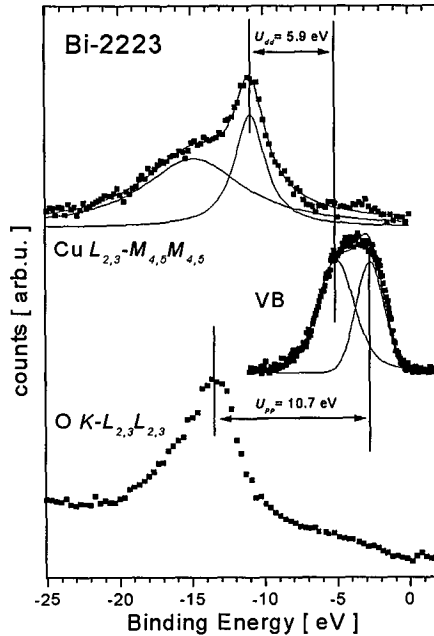


Fig. 5. The valence band Cu 3*d* and O 2*p* emissions along with the Cu: $L_{2,3}-M_{4,5}M_{4,5}$ and of O $K-L_{2,3}L_{2,3}$ Auger spectra with their respective Fermi energies aligned and the U_{dd} and U_{pp} energies as indicated.

The energy difference between the valence band copper emission and the high energy peak *A* in the Cu $L_{2,3}-M_{4,5}M_{4,5}$ Auger spectrum provides us with an estimate of $U_{dd} \cong 5.9 \pm 0.5$ eV. The energy difference between the valence band oxygen emission and the O $K-L_{2,3}L_{2,3}$ Auger line gives an estimate of $U_{pp} \cong 10.4 \pm 1$ eV. We can use here an additional relation $U_{cd} \cong 1.4U_{dd}$ which is consistent with a large body of experimental results. From this we have $U_{cd} = 8.3 \pm 0.5$ eV. Finally, we can compare the relevant copper/oxygen VB emission with oxygen/copper Auger line, respectively. This procedure gives an estimate $U_{cd} = U_{dc} = 8.3 \pm 1$ eV which is the same as the previous one. The error is due to the accuracy of the alignment of the relevant Auger lines to the Fermi energy.

Also the structure of the Cu $L_{2,3}-M_{4,5}M_{4,5}$ Auger line for copper compounds may be analyzed according to the model presented in [8]. The main peak *A* is due to a correlated two-hole final state and the shoulder *B* is due to transitions into the uncorrelated two-hole final state. The line *A* was attributed to the $3d^8L^{-1}$ final state configuration after the Auger process starting from a $2p_{3/2}3d^{10}L^{-1}$ intermediate state. The line *B* was assigned to the $3d^7$ final configuration from a $2p_{3/2}3d^9$ intermediate state [8]. It was calculated [8] that

$$E_A - E_B \cong 2U_{dd} - U_{cd} \quad (1)$$

and this relation was used in the estimation of U_{cd} . Having the value of U_{dd} one can calculate the value of U_{cd} taking into account the above relation and the experimental value of $E_A - E_B \cong 4.0 \text{ eV} \pm 0.3 \text{ eV}$ (c.f. the Table and Fig. 4). Hence $U_{cd} = 7.9 \pm 0.5 \text{ eV}$.

The estimations of U_{dd} , U_{pp} , and U_{cd} are in agreement with the estimates of the same quantities of other copper oxide superconductors and strongly correlated copper compounds [14, 32].

3.2. Analysis of charge transfer satellites

As it was said the two possible VB excitations are possible. The first $d-d$ excitation needs the energy $U_{dd} = E(d^{n+1}) + E(d^{n-1}) - 2E(d^n)$. The second excitation from p -ligand ion (configuration L) onto the d^n configuration of a metal ion needs the energy $\Delta = E(d^{n+1}) + E(L^{-1}) - E(d^n) - E(L)$. Creation of a core hole shifts the $d^{n+1}L^{-1}$ but not d^nL configuration down by an amount U_{cd} so that the difference between the satellite line and the main line is $\Delta E_{M-S} = (U_{cd} - \Delta)$ depending on the relative magnitude of U_{cd} and Δ . If one takes into consideration the hybridization effect between the metal ions and the ligand ions a more general description which is applicable to any d^n configuration was elaborated in [8-10]. From this approach one can elaborate the photoemission spectra. Especially, the satellite to the main peak energy distance in the Cu $2p$ core-level XP spectra is expressed as [8]

$$\Delta E_{M-S} \cong \sqrt{(U_{cd} - \Delta)^2 + 4T_m^2} = \sqrt{(U_{cd} - \Delta)^2 + 4t^2}, \quad (2)$$

where the mixing matrix element between the two initial states $\Delta = E(3d^{10}L^{-1}) - E(3d^9)$ is given by $T_m = \langle 3d^9 | H | 3d^{10}L^{-1} \rangle \cong t$.

For the analysis of the experimental satellite data according to the above formulae one needs other quantitative estimates of two quantities out of Δ , U_{cd} , and t . Now we can use the value of $U_{cd} = 8.3 \text{ eV}$ which has been just estimated in the previous paragraph. In addition according to the previous paragraph $\Delta E_{A-B} \cong 2U_{dd} - U_{cd} = 4.5 \pm 0.5 \text{ eV}$ from the Auger spectra just analyzed above. Hence, taking the value of $U_{dd} = 5.9 \pm 0.5 \text{ eV}$ from the previous paragraph we have for $U_{cd} = 7.9 \pm 0.5 \text{ eV}$ as an additional estimate. The relative size of Δ and U_{cd} determines whether in a TM compound with configuration d^nL in the initial state after photoionization the same d^nL configuration is the lowest final state or whether the $d^{n+1}L^{-1}$ configuration is the final state. This model forms the basis for analysis photoemission data. Hence, taking into account the above formulae one can estimate the values of t assuming that Δ is about 1.5 eV which is again consistent with a large number of experimental results and theoretical calculations [14-34]. Thus a complete set of parameters is

$$U_{dd} = 5.9 \pm 0.5 \text{ eV}, \quad U_{cd} = 7.9 \pm 0.5 \text{ eV},$$

$$U_{pp} \cong 10.4 \pm 1 \text{ eV} \quad \text{and} \quad t = 1.3 \pm 0.5 \text{ eV},$$

for $\Delta = 1.5 \text{ eV}$. From these values the investigated superconductors must be classified as the charge transfer strongly-correlated hole-type metals according to Zaanen-Sawatzky-Allen (ZSA) phase diagram [2]. An additional argument for the charge transfer behavior of these compounds is the majority contribution from the oxygen $2p$ emission to the top of valence band (c.f. Fig. 3).

4. Summary and conclusions

1. Our XPS, UPS, and Auger spectra of $(\text{Tl}_{0.6}\text{Pb}_{0.5})(\text{Sr}_{0.9}\text{Ba}_{0.1})_2\text{Ca}_2\text{Cu}_3\text{O}_y$ and $(\text{Bi}_{1.75}\text{Pb}_{0.35})\text{Sr}_{1.9}\text{Ca}_{2.05}\text{Cu}_{3.05}\text{O}_y$ superconductors were assigned to the photoemission electronic final state configurations according to the standard approach for copper compound and the great number of spectroscopic results collected up to now. We have observed the Fermi edge in the valence band of the bismuth superconductor which was a very good reference energy for analysis of the recorded spectra.
2. From the energy difference between the Cu valence band emission and the high energy peak *A* of the Cu $L_{2,3}\text{-}M_{4,5}M_{4,5}$ Auger spectrum the on-site $d\text{-}d$ Coulomb correlation energy was estimated to be $U_{dd} \cong 5.9 \pm 0.5$ eV. The energy difference between the oxygen valence band emission and the O $K\text{-}L_{2,3}L_{2,3}$ Auger line gives an estimate of the on-site $p\text{-}p$ Coulomb correlation energy $U_{pp} \cong 10.4 \pm 1$ eV. From the energy separation between the two components of the Cu $L_{2,3}\text{-}M_{4,5}M_{4,5}$ Auger line the $2p$ core hole - $3d$ hole correlation energy was calculated to be $U_{cd} = 7.9 \pm 0.5$ eV.
3. The hopping integral $t = 1.3 \pm 0.5$ eV was extracted from the satellite to the main peak energy distance in the Cu $2p$ core-level XP spectra and assuming the charge transfer energy to be $\Delta = 1.5$ eV.
4. These correlation energies and the relative magnitude of $U_{dd} > \Delta$ define that both superconductors are the charge transfer strongly-correlated hole-type metals according to the phase diagram U_{dd}/t versus Δ/t [2].

Acknowledgments

This study was financially supported by the Committee for Scientific Research (Poland) (project No. 2P03B 147 17), and by the Österreichischer Akademischer Austauschdienst, Wissenschaftlich-technische Zusammenarbeit mit Polen (project 3/99). We thank Prof. A. Szytuła and Mr. B. Penc for making possible the photoemission experiments in the Institute of Physics of the Jagiellonian University in Cracow.

References

- [1] N.F. Mott, J.H. Davies, *Electronic Processes in Non-Crystalline Materials*, Oxford University Press, Oxford 1979, p. 197.
- [2] J. Zaanen, G.A. Sawatzky, J.W. Allen, *Phys. Rev. Lett.* **55**, 418 (1985).
- [3] G.A. Sawatzky, J.W. Allen, *Phys. Rev. Lett.* **53**, 2339 (1984).
- [4] J. Zaanen, G.A. Sawatzky, *J. Solid State Chem.* **88**, 8 (1990).
- [5] H. Eskes, G.A. Sawatzky, *Phys. Rev. B* **43**, 119 (1991).
- [6] T. Bandyopadhyay, D.D. Sarma, *Phys. Rev. B* **39**, 3517 (1989).
- [7] A. Fujimori, F. Minami, S. Sugano, *Phys. Rev. B* **29**, 5225 (1984).

- [8] G. van der Laan, C. Westra, C. Haas, G.A. Sawatzky, *Phys. Rev. B* **23**, 4369 (1981).
- [9] S. Asada, S. Sugano, *J. Phys. Soc. Jpn.* **41**, 1291 (1976).
- [10] M.A. van Veenendaal, G.A. Sawatzky, *Phys. Rev. B* **49**, 3473 (1994).
- [11] Z.-X. Shen, J.W. Allen, J.J. Yeh, J.-S. Kang, W. Ellis, W. Spicer, I. Landau, M.B. Maple, Y.D. Dalichaouch, M.S. Torikachvili, J.Z. Sun, T.H. Geballe, *Phys. Rev. B* **36**, 8414 (1987).
- [12] J. Ghijsen, G.A. Sawatzky, M.T. Czyzyk, *Phys. Rev. B* **38**, 11322 (1988).
- [13] G. Chiaia, M. Qvarford, I. Lindau, S. Söderholm, U.O. Karlsson, S.A. Flodström, L. Leonyuk, A. Nilsson, N. Mårtensson, *Phys. Rev. B* **51**, 1213 (1995).
- [14] S. Hüfner, *Photoelectron Spectroscopy*, in *Springer Series in Solid-State Sciences*, Vol. 82, Springer-Verlag, Berlin 1995, p. 226 and references cited therein.
- [15] for early review see A. Bianconi, in: *Proc. the Taniguchi Int. Symposium on Core Level Spectroscopy in Condensed System*, Eds. A. Kotani, J. Kanamori, Springer Verlag, Berlin 1989, p. 99.
- [16] A. Kołodziejczyk, *Mol. Phys. Report* **15/16**, 11 (1996) and references cited therein.
- [17] P. Steiner, S. Hüfner, V. Kinsinger, I. Sander, B. Siegwart, H. Schmitt, R. Schulz, S. Junk, G. Schwitzgebel, A. Gold, C. Politis, H.P. Müller, R. Hoppe, S. Kemmler-Sack, C. Kunz, *Z. Phys.* **B69**, 449 (1988).
- [18] For review see *Fermiology of High-T_c Superconductors*, Eds. A. Bansil, A.J. Arko, R. Benedek, V.J. Emery, L.C. Smedskjaer, *J. Phys. Chem. Solids* **52**, (1991).
- [19] For review see *Electronic Structure and Fermiology of High-T_c Superconductors*, Eds. T. Takahashi, A. Bansil, H. Katayama-Yoshida, *J. Phys. Chem. Solids* **53**, (1992).
- [20] J.C. Campuzano, G. Jennings, M. Faiz, L. Beaulaigue, B.W. Veal, J.Z. Liu, A.P. Paulikas, K. Vandervoort, H. Claus, R.S. List, A.J. Arko, R.J. Barlett, *Phys. Rev. Lett.* **64**, 2308 (1990).
- [21] R. Manzke, G. Mante, R. Claessen, M. Skibowski, J. Fink, *Surf. Sci.* **269**, 1066 (1992).
- [22] R. Liu, B.W. Veal, A.P. Paulikas, J.W. Downey, H. Shi, C.G. Olson, C. Gu, A.J. Arko, J.J. Joyce, *Phys. Rev. B* **45**, 5614 (1992).
- [23] J.G. Tobin, C.G. Olson, C. Gu, J.Z. Liu, F.R. Solal, M.J. Fluss, R.H. Howell, J.C. O'Brien, H.B. Radousky, P.A. Sterne, *Phys. Rev. B* **45**, 5563 (1992).
- [24] J.C. Campuzano, K. Gofron, R. Liu, H. Ding, B.W. Veal, B. Dabrowski, *J. Phys. Chem. Solids* **53**, 1577 (1992).
- [25] A.A. Abrikosov, J.C. Campuzano, K. Gofron, *Physica C* **214**, 73 (1993).
- [26] D.S. Dessau, Z.-X. Shen, B.O. Wells, W.E. Spicer, A.J. Arko, *J. Phys. Chem. Solids* **52**, 1401 (1992).
- [27] R.O. Anderson, R. Claessen, J.W. Allen, C.G. Olson, C. Janowitz, L.Z. Liu, H.-H. Park, M.B. Maple, Y. Dalichaouch, M.C. de Andrade, R.F. Jarodim, E.A. Early, S.-J. Oh, W.P. Ellis, *Phys. Rev. Lett.* **62**, 336 (1988); *Phys. Rev. Lett.* **70**, 3163 (1993).
- [28] W. König, G. Gritzner, M. Reissner, W. Steiner, *Physica C* **258**, 175 (1996).
- [29] M. Mair, W. König, G. Gritzner, *Supercond. Sci. Technol.* **8**, 894 (1995).

- [30] W. König, G. Gritzner, P. Diko, J. Kovác, M. Timko, *J. Mater. Chem.* **5**, 879 (1995); W. König, M. Mair, G. Gritzner, *J. Supercond.* **11**, 107 (1998).
- [31] Z.-X. Shen, D.S. Dessau, *Phys. Rep.* **253**, 1 (1995).
- [32] R. Zimmermann, Ph.D. Thesis, Universität des Saarlandes, Saarbrücken 1996.
- [33] S. Tougaard, *Surf. Sci.* **216**, 343 (1989).
- [34] A. Chainani, M. Mathew, D.D. Sarma, *Phys. Rev. B* **46**, 9976 (1992).